

Preparation and Study of Decavanadate-Pillared Hydrotalcite-like Anionic Clays Containing Transition Metal Cations in the Layers. 2. Samples Containing Magnesium–Chromium and Nickel–Chromium

F. Kooli,^{†,‡} V. Rives,^{*,†} and M. A. Ulibarri[‡]

Departamento de Química Inorgánica, Facultad de Farmacia, Universidad de Salamanca, 37007-Salamanca, Spain, and Departamento de Química Inorgánica e Ingeniería Química, Facultad de Ciencias, Universidad de Córdoba, 14004-Córdoba, Spain

Received January 10, 1995[®]

Mg–Cr and Ni–Cr layered double hydroxides (LDHs) with carbonate anions in the interlayer were used as precursors to synthesize pillared derivatives with decavanadate ($V_{10}O_{28}^{6-}$) anions without the use of any preswelling agent. Characterization was carried out by powder X-ray diffraction, chemical analysis, FT-infrared spectroscopy, thermal analysis, and transmission electron microscopy. The influence of the wetness degree of the starting Mg–Cr and Ni–Cr LDHs and of the pH conditions on the anionic-exchange rate of carbonate was studied. The pillared materials were constituted by a well crystalline phase, together with a coproduct with a lower degree of crystallinity, characterized by a broad X-ray diffraction peak close to 10 Å. Anion-exchange was neither achieved without prewetting of the carbonate-containing LDH nor at pH values larger than 6.5. The thermal stability of the pillared materials and their surface properties are also presented.

Introduction

A new class of materials based on pillared smectite clays in which the pillaring species are polymeric cations, has been reported.¹ The polymeric cations are thermally stable, and the resulting porous solids could be useful as catalysts and photocatalysts. Layered double hydroxides (LDHs), the so-called anionic clays, have high exchange capacities, in the range 2.4–4.1 mequiv/g depending upon their exact composition. Exploiting their ion-exchange properties and using polyoxometalates (POMs) as pillaring species, as has been demonstrated for cationic clays, leads to pillared LDHs. These are potentially thermally stable materials with interesting porosity properties.^{2,3} The strategies described in the literature for their synthesis make use of the fact that chloride or nitrate anions are significantly easier to displace than carbonate. Kwon et al.² have reported the use of the chloride form of an LDH to exchange for decavanadate ($V_{10}O_{28}^{6-}$), whilst Woltermann³ used the nitrate form to exchange for numerous polyoxometalate anions including $Ta_6O_{18}OH^{7-}$, $Nb_6O_{18}OH^{7-}$, $V_{10}O_{28}^{6-}$, $PMo_6V_6O_{40}^{3-}$, etc. Drezdson⁴ has relied upon the use of LDH initially synthesized with a large organic anion as the intercalated species; the organic anion is subsequently displaced by the polyoxometalate species. Using a sort of *effect memory*, LDHs calcined at intermediate temperatures (ca. 250–350 °C) can rehydrate to incorporate anions, and reconstruct the original LDH structure;⁵ the method has been successfully used to obtain a variety of materials with organic and inorganic anions in the interlayer.^{6–9}

The anion-exchange properties of LDHs have been examined by Miyata¹⁰ and other authors, who found the carbonate anion to be the most selective and tenaciously held within the layers and thus difficult to exchange.

To our knowledge, the direct synthesis of LDHs pillared with decavanadate and other POM anions, via anion exchange from carbonate-containing LDHs as a precursor, has not been reported in the literature. Anion exchange of nitrate by polyoxometalates without the use of any preswelling agent has been reported by Wang et al.¹¹

We have previously reported the synthesis of a Ni–Al–CO₃ LDH with decavanadate as pillaring agent,^{9,12} and in the present paper we report for the first time the synthesis of decavanadate-containing LDHs with Mg–Cr and Ni–Cr in the brucite-like layers and carbonate anions in the interlayer space, without preswelling, but keeping the fresh material wet before exchange.¹³ The characterization of the new materials and their physicochemical properties are also reported.

Experimental Section

Samples Preparation. Ni–Cr, and Mg–Cr LDHs (hereafter NiCrCO₃ and MgCrCO₃, respectively) were prepared by coprecipitation using a technique similar to that described by Reichle.¹⁴ All chemicals were from Fluka (Germany). A 250 mL aliquot of an aqueous solution containing 0.1 mol of nickel (or magnesium) nitrate and 0.05 mol of chromium nitrate was added dropwise to a vigorously stirred aqueous solution, kept at 65 °C, formed by dissolving 0.7 mol of NaOH and 0.2 mol of Na₂CO₃ in 200 mL of water (pH ca. 11). Addition took along ca. 30 min. The obtained gel was aged overnight and then separated by centrifugation and washed with distilled water. The slurry

[†] Universidad de Salamanca.

[‡] Universidad de Córdoba.

[®] Abstract published in *Advance ACS Abstracts*, September 15, 1995.

- (1) Pillared Clays. In *Catalysis Today*; Burch, R., Ed.; Elsevier: Amsterdam, 1988; Vol. 2.
- (2) Kwon, T.; Tsigdinos, G. A.; Pinnavaia, T. J. *J. Am. Chem. Soc.* **1988**, *110*, 3653.
- (3) Woltermann, G. M. U.S. Patent 4,454,244, 1988.
- (4) Drezdson, M. A. *Inorg. Chem.* **1988**, *27*, 4628.
- (5) Sato, T.; Fujita, H.; Endo, T.; Shimada, M.; Tsunashima, A. *React. Solids*. **1988**, *5*, 219.
- (6) Chibwe, K.; Jones, W. *Chem. Mater.* **1989**, *1*, 489.
- (7) Chibwe, K.; Jones, W. *J. Chem. Soc., Chem Commun.* **1989**, 926.

- (8) Ulibarri, M. A.; Labajos, F. M.; Rives, V.; Trujillano, R.; Kagunya, W.; Jones, W. *Inorg. Chem.* **1994**, *33*, 2592.

- (9) Kooli, F.; Rives, V.; Ulibarri, M. A. *Mater. Sci. Forum* **1994**, *152–153*, 375.

- (10) Miyata, S. *Clays Clay Miner.* **1983**, *31*, 305.

- (11) Wang, T.; Tian, Y.; Wang, R.-C.; Colon, J.; Clearfield, A. *Chem. Mater.* **1992**, *4*, 1276.

- (12) Kooli, F.; Rives, V.; Ulibarri, M. A. *Inorg. Chem.* **1995**, *34*, 5114.

- (13) Carrado, K. A.; Forman, J. E.; Botto, R. E.; Winans, R. E. *Chem. Mater.* **1993**, *5*, 472.

- (14) Reichle, W. T. *J. Catal.* **1985**, *94*, 547.

Table 1. Chemical Analyses of Parent MgCrCO₃ and NiCrCO₃ Samples and of Decavanadate-Pillared Samples Obtained at pH = 4.5

Sample	% Mg	% Ni	% Cr	% V	% C	Mg/Cr ^a	Ni/Cr ^a	V/Cr ^a
NiCrCO ₃		56.4	12.6		1.0		4.0	
MgCrCO ₃	21.3		20.7		2.0	2.2		
NiCrV		22.3	10.0	16.3			2.0	1.7
MgCrV	9.7		15.9	18.2		1.3		1.1

^a Atomic ratio.

was hydrothermally treated at 120 °C for 48 h, and part was dried at 80 °C in air (dried samples, D) and another other part was kept in suspension as a slurry (slurry samples, S).

A 6 g sample of sodium (meta)vanadate from Fluka was dissolved in 100 mL of distilled water. The pH was adjusted with a Metrohm Dosimat 725, using a 0.5 M HCl solution. Before addition of the metavanadate solution, the pH of the slurry suspension (either the original slurry, samples S, or one obtained by suspending three grams of the dried LDH, samples D, in 300 mL of water overnight to ensure complete wetting of the solid particles) was also adjusted at 4.5 (which was maintained along all the addition and stirring periods), then the metavanadate was added dropwise to the Ni–Cr (or Mg–Cr) suspension, and the suspension thus obtained was stirred for 96 h at room temperature. The yellow precipitate was separated by centrifugation, washed, and dried at 70 °C. Samples are designated as NiCrV and MgCrV, respectively.

Other series of samples were prepared at pH values ranging from 4.5 to 8.5.

Characterization. Powder X-ray diffraction (PXRD) profiles were obtained using a Siemens diffractometer with Cu K α radiation and graphite monochromator. Ni, Mg, Cr, and V analyses were carried out by atomic absorption in a Perkin-Elmer atomic absorption spectrometer, Model 3100, after dissolution of the product in a HCl solution. Carbon analysis was carried out in a Perkin-Elmer 2400 CHN analyzer. Differential thermal analysis (DTA) and thermogravimetric analysis (TG) of the samples were carried out in Perkin-Elmer DTA 1700 and TGS-2 apparatuses, respectively, coupled to a Perkin-Elmer 3600 data station, at a heating rate of 10 °C/min. The FT-IR spectra were recorded in a BOMEN MB-100 spectrometer in the 6000–400 cm⁻¹ range using pressed KBr pellets. Microstructural characterization of the materials was carried out in a JEOL 200CX transmission electron microscope.

Full nitrogen adsorption/desorption isotherms at –196 °C for surface area and porosity assessment were measured in a conventional Pyrex high-vacuum system equipped with a MKS pressure transducer, grease-free stopcocks, an APV-DD4 rotatory pump, and a silicon oil diffusion pump.

Results and Discussion

Chemical Analysis. The chemical analysis data for the samples are summarized in Table 1.

The M²⁺/Cr³⁺ ratios are lower in the decavanadate-containing samples than in the starting materials. The difference is due to an easier dissolution of Mg²⁺ and Ni²⁺ than the more acidic Cr³⁺ cation under the experimental conditions during preparation of the POM-exchanged samples. Although some other polyoxovanadate species can be formed, depending on the pH range, results below indicate the polymerization has led to formation of the decavanadate (V₁₀O₂₈⁶⁻) anion. The V/Cr atomic ratio should be 1.66. For sample NiCrV this ratio is 1.7, in good agreement with the expected value. However, for sample MgCrV the value is only 1.14. This difference may be related to the formation of a larger amount of less crystalline coproduct (see X-ray diffraction data below).

X-ray Diffraction. Ni–Cr–V samples. Powder X-ray diffraction diagrams for a series of Ni–Cr samples are shown in Figure 1. Pattern 1a corresponds to sample NiCrCO₃, and shows well-defined maxima at 7.61, 3.78, and 2.58 Å that, upon comparison with the patterns of different layered hydroxycar-

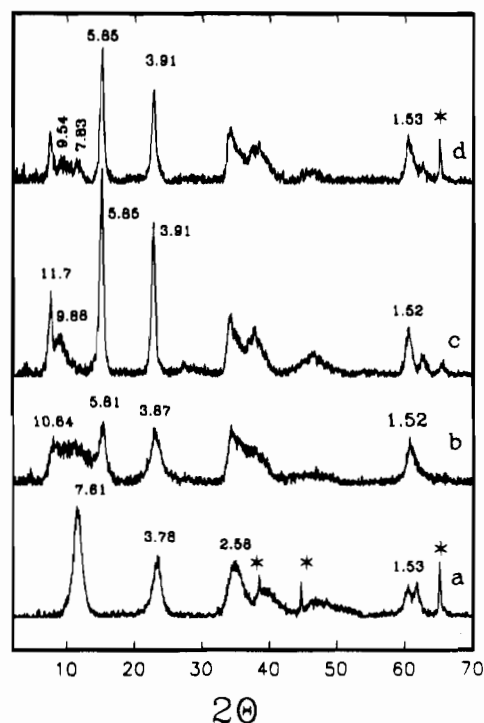


Figure 1. PXRD diagrams: (a) parent NiCrCO₃ anionic clay; (b) sample NiCrV prepared by addition of decavanadate solution to a suspension of sample NiCrCO₃-D at pH = 4.5; (c) sample NiCrV prepared by addition of decavanadate solution to a suspension of sample NiCrCO₃-S at pH = 4.5; (d) same sample at pH = 5.5 (* = peaks due to the Al sample holder.)

bonates with the hydrotalcite-like structure,¹⁵ can be ascribed to diffraction by planes (003), (006), and (009) (or (012)). *d*(003) (7.61 Å) coincides very well with the values reported for other samples also containing carbonate as the interlayer anion. Dimension *a* of the crystal can be calculated as twice the position of the peak originated by diffraction by planes (110), here recorded at 1.53 Å.

If the dried NiCrCO₃ sample (NiCrCO₃-D) is added to the vanadate solution at pH = 4.5, the solid isolated is observed to be fairly uncrystalline, and the PXRD pattern demonstrates that no exchange has been attained, the peaks being recorded in the same positions as for sample NiCrCO₃. It could be argued that exchange with chloride anions from the solution has occurred, but FT-IR data below indicate that carbonate anions persist in the sample.

If sample NiCrCO₃-D is suspended in water at pH = 4.5 and stirred overnight at room temperature before addition of the vanadate solution (also at pH = 4.5), the PXRD pattern, Figure 1b, shows development of a peak at 5.81 Å, a position close to that reported in the literature^{2,4} for diffraction by planes (006) of decavanadate-exchanged LDHs. However, the peak corresponding to diffraction by planes (003), expected at 11.62 Å, is not recorded, and instead a broad feature extending along a fairly wide 2θ range is recorded. Carbonate species have been completely removed from the interlayer space, as no peak is recorded close to 7.6 Å, and the hydrotalcite-like structure of the material is maintained, as shown by detection of the (110) plane at 1.52 Å, the value being slightly lower than that for parent NiCrCO₃ due to the lower Ni²⁺ content (the value of *a* is related to the ionic radii of the cations in the layers).¹⁶

However, when the synthesis is carried out in the same way, but using sample NiCrCO₃-S (i.e., that not dried, but maintained

(15) Cavani, F.; Trifiró, F.; Vaccari, A. *Catal. Today* 1991, 11, 173.

(16) Brindley, G. W.; Kikkawa, S. *Clays Clay Miner.* 1980, 28, 87.

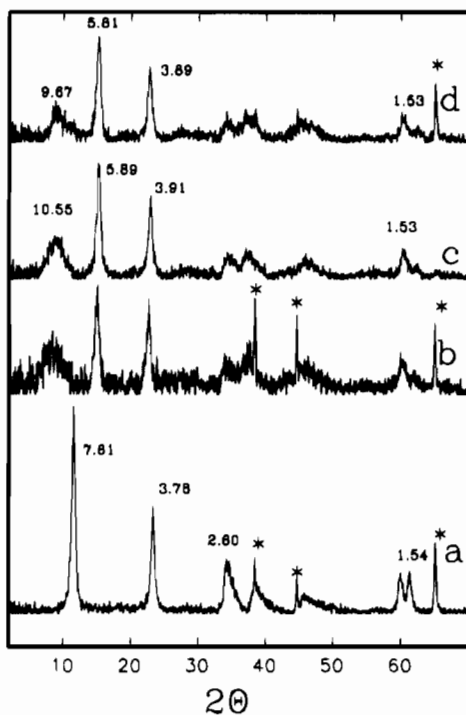


Figure 2. PXRD diagrams: (a) parent MgCrCO_3 anionic clay; (b) sample MgCrV prepared by addition of decavanadate solution to a suspension of sample $\text{MgCrCO}_3\text{-S}$ at $\text{pH} = 4.5$; (c) sample MgCrV prepared by addition of decavanadate solution to a suspension of sample $\text{MgCrCO}_3\text{-S}$ at $\text{pH} = 4.5$; (d) same sample at $\text{pH} = 5.5$ (* = peaks due to the Al sample holder.)

in a slurry after preparation), rather different results are obtained. Together with the (110) peak at 1.52 \AA , sharp peaks are recorded at 5.85 and 3.91 \AA , planes (006) and (009), the (003) signal now being recorded as a weak, but sharp and clearly defined peak at 11.69 \AA , although, again, a broad feature centered at 9.88 \AA is recorded, Figure 1c. So, two phases seem to be present, a layered one and a second one, responsible for the broad peak at 9.88 \AA ; no indication of the presence of carbonate-containing layered material is recorded. Probably, a rather low swelling ability of sample $\text{NiCrCO}_3\text{-D}$ avoids an easy exchange of carbonate by decavanadate anions, as previously reported for NiAlCO_3 LDH.¹² The weak broad peak around 9.8 \AA has been also reported by several studies^{8,17} and was attributed to divalent and trivalent salts of polyoxometalate in the case of Zn–Al pillared LDHs by $(\alpha\text{-SiW}_{11}\text{O}_{39})^{8-}$ and $(\alpha\text{-1,2,3-SiV}_3\text{W}_9\text{O}_{40})^{7-}$ anions.

For pH larger than 5.5 no exchange occurs, the patterns being coincident with that shown in Figure 1a for sample NiCrCO_3 . At $\text{pH} = 5.5$, however, a partial exchange seems to take place, diffraction maxima due to the decavanadate-containing solid being recorded at 5.85 and 3.91 \AA , while traces of the original, carbonate-containing sample gives rise to the weak peak at 7.83 \AA , Figure 1d.

Assuming the thickness of the brucite layer to be 4.8 \AA ,¹⁸ the interlayer distance, as calculated from $d(003)$, is close to 6.9 \AA , corresponding to $(\text{V}_{10}\text{O}_{28})^{6-}$ anion with an orientation in which the C_2 axis is parallel to the host layers.^{2,4}

Mg–Cr–V Samples. A study parallel to that above described for samples containing Ni,Cr, but for samples Mg,Cr has been also carried out, the PXRD data being shown in Figure 2. For the original MgCrCO_3 LDH material, Figure 2a, diffractions by basal planes are recorded at 7.61 , 3.78 , and 2.60

\AA , the (110) plane being responsible for the peak at 1.54 \AA . The three sharp peaks close to 40 , 45 , and 65° (2θ) are due to the aluminum sample holder used to record the PXRD profiles.

As for the Ni,Cr system, direct exchange of decavanadate with sample $\text{MgCrCO}_3\text{-D}$ did not occur, spacings for the broader recorded peaks being almost coincident to those of the original carbonate-containing solid. If sample $\text{MgCrCO}_3\text{-D}$ is previously stirred overnight, exchange takes place, although leading to a poorly crystallized material, with weak X-ray diffractions at 5.89 and 3.91 \AA due to planes (006) and (009) and also the broad feature at 10.55 \AA . The use of the slurry sample, $\text{MgCrCO}_3\text{-S}$, leads to formation of a well crystallized material, with basal diffraction maxima, Figure 2b, at 5.82 and 3.89 \AA , the (110) diffraction peak at 1.53 \AA , and again the broad peak at 10.25 \AA . However, it should be noted that in this case the peak due to diffraction by planes (003) of the decavanadate-intercalated solid, expected at 11.64 \AA , is not recorded. This peak is rather low in the diffraction pattern recorded for sample NiCrV prepared following the same procedure, and so it can be assumed that in the case of the Mg,Cr system it is obscured by the broad diffraction at 10.25 \AA . It should be pointed out that the relative intensity of the peak due to diffraction by the (006) planes of the layered material, if compared to that of the broad peak at ca. 10 \AA , is larger for the system Ni,Cr, which can be tentatively taken as an indication of a large amount of the coproduct in the system Mg,Cr. So, although this coproduct, responsible for the broad feature close to 10 \AA , is formed in different LDH systems intercalated with different POMs, whatever the nature of the divalent and trivalent cations in the brucite-like layers, the relative intensity and the broadness of this peak seems to be dependent on the nature of such cations.^{8,12}

When pH is increased, the results obtained are similar to those with sample NiCrV , although in this case the maximum pH at which exchange was attained was 6.5 .

It appears that the ability of the LDH structure to undergo $\text{CO}_3^{2-}/\text{V}_{10}\text{O}_{28}^{6-}$ exchange depends both on the pH and on the nature of the cations in the host structure.

Mendiboure and Schollhorn¹⁹ have reported that for $\text{Ni}^{2+}/\text{Fe}^{3+}$ and $\text{Ni}^{2+}/\text{Co}^{3+}$ systems the carbonate/chloride exchange takes place in a few minutes at $\text{pH} \leq 5$; such a fast exchange has been also found by us for the Ni,Al system.¹² Chloride is more easily replaced than carbonate,¹⁰ and then chloride is exchanged by $\text{V}_{10}\text{O}_{28}^{6-}$.

Although the exact effect of the nature of the layer cations on the facility of exchange at different pH s remains unclear, total exchange was achieved at $\text{pH} = 5.5$ in the systems Ni,Al, Ni,Cr, and Mg,Cr; at $\text{pH} = 6.5$ total exchange was achieved for Mg,Cr, while for Ni,Al only a partial exchange occurred, and no exchange at all was observed for Ni,Cr. Contrary to the results reported by Twu and Dutta²⁰ for the lithium–aluminum nitrate, no decrease in the polymerization degree of the intercalated polyvanadate was observed as the pH was raised.

Thermal Analysis. NiCrCO₃ and Ni–Cr–V Samples. The TG and DTA diagrams of the starting $\text{NiCrCO}_3\text{-D}$ sample, recorded in air and in nitrogen, are shown in Figure 3A. Although in some LDHs decomposition takes place in three consecutive steps,²¹ leading to plateaus in the TG diagram, in this case the first and second weight losses are overlapped. The corresponding DTA profile shows three minima at 139 , 223 , and $366 \text{ }^\circ\text{C}$; weight loss up to ca. $420 \text{ }^\circ\text{C}$ (where the third DTA minimum has been completed) represents 31% of the initial

(19) Mendiboure, A.; Schollhorn, R. *Rev. Chim. Miner.* **1986**, *23*, 819.

(20) Twu, J.; Dutta, K. *J. Phys. Chem.* **1989**, *23*, 7863.

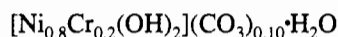
(21) Pesic, L.; Salipurovic, S.; Markovic, V.; Kagunya, W.; Jones, W. J. *Mater. Chem.* **1992**, *2*, 1069.

(17) Narita, E.; Kaviratna, P.; Pinnavaia, T. J. *Chem. Lett.* **1991**, 805.

(18) Allmann, R. *Acta Crystallogr., Sect. B* **1968**, *24*, 972.

sample weight. The remaining weight loss up to 750 °C corresponds only to 4% (3% when the analysis was performed in nitrogen) of the initial weight and is due to removal of strongly held hydroxyl groups. The DTA profile recorded in air shows also a weak, broad endothermic effect between 445 and 600 °C, absent in the profile recorded in nitrogen. This behavior indicates that such an effect is undoubtedly related to an oxidation (or reduction) process. Such an effect has been reported previously^{22–24} for systems similar to that here studied, also containing Cr³⁺ cations in the layers. For Mg,Cr systems it has been reported that calcination in air leads to intermediate formation of Cr⁶⁺-containing species that at higher temperatures are again reduced to the Cr³⁺ state, forming MgCr₂O₄;²⁵ similar conclusions have been reached by using FT-IR spectroscopy for Ni,Cr systems.^{26,27}

From the chemical analysis data in Table 1 and the quantitative thermogravimetric analysis, the following formula can be calculated for this sample:



The TG and DTA of the Ni–Cr–V material are shown in Figure 3B. The shape is similar to that of the starting material, without differentiation of the steps during decomposition. As previously reported for Ni,Al–V₁₀O₂₈^{6–} systems,¹² the carbonate/decavanadate exchange leads to removal of the endothermic peak at 366 °C; effects due to removal of water are now recorded at 107 and 180 °C, with weaker endothermic effects at 287 and 398 °C. Total weight loss up to 440 °C was only 20%, lower than that for sample NiCrCO₃-D, due to the fact that vanadate-containing species are not removed during calcination, as carbonate species were. The very weak exothermic effects recorded between 500–700 °C should be originated by reaction of the layer cations with decavanadate-derived species, leading mainly to Ni₃V₂O₈, as confirmed by X-ray diffraction analysis of the residue after the thermal analysis.

MgCrCO₃ and Mg–Cr–V Samples. The TG/DTA profiles for sample MgCrCO₃-D are shown in Figure 4A. As previously reported for many other LDHs systems, the first weight loss, due to removal of molecular water, is here clearly defined, and extends from room temperature up to 250 °C. The weight loss in this temperature range corresponds to 16% of the initial sample weight and can be correlated to two endothermic effects at 118 and 240 °C. The next weight loss, up to 450 °C, corresponds to 19% of the initial weight, and can be ascribed to removal of hydroxyl groups from the layers and carbon dioxide from carbonate species in the interlayer space; such a weight loss corresponds to the broad endothermic DTA peak at 399 °C, where a shoulder at ca. 365 °C can be distinguished. Final weight loss up to 750 °C represents only ca. 5% of the initial sample weight. The endothermic effect due to the redox process of the chromium ions is recorded in air at 580 °C, and is absolutely absent in the profile recorded in nitrogen.

From the chemical analysis for this sample in Table 1 and the weight loss up to 250 °C (due to water removal), the formula

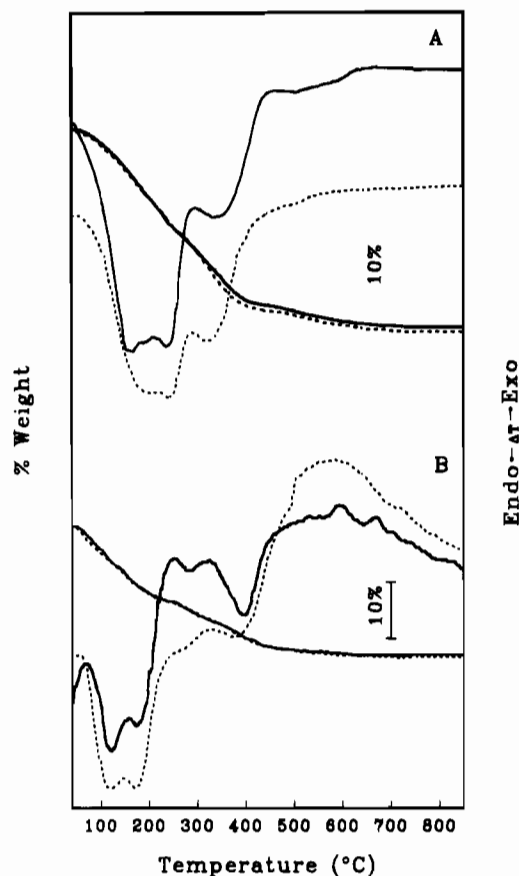
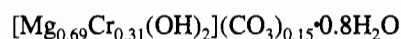


Figure 3. (A) Thermogravimetric and differential thermal analysis curves for sample NiCrCO₃-D recorded in air (solid line) and in nitrogen (dotted line). (B) Thermogravimetric and differential thermal analysis curves for sample NiCrV recorded in air (dotted line) and in nitrogen (solid line).

of this material can be written as follows:



From this formula, the calculated weight of the residue after calcination would be 62%, reasonably coincident with the experimentally determined value of 60%.

Results of the thermal analysis for sample Mg–Cr–V are shown in Figure 4B. The three steps are fairly well defined in the TG profile, both when recorded in air and in nitrogen. Molecular water loss is recorded up to ca. 200 °C and represents 14% of the initial weight loss. The corresponding endothermic peaks in the DTA profile are recorded at 125 and 207 °C. The next endothermic peak is much weaker than for sample MgCrCO₃-D, as expected due to removal of hydroxyl groups only, and is recorded at 408 °C. In both cases, an exothermic peak at 673–677 °C should be due to a recrystallization process, probably leading to Mg(Cr)-V–O compounds.

FT-IR Spectroscopy. The technique has been used mainly to identify the nature of the interlayer anion. The spectra for all four samples are shown in Figure 5. The broad absorption between 3600–3300 cm⁻¹ is due to stretching mode of hydrogen-bonded hydroxyl groups, both from the brucite-like layers and from the interlayer water molecules. The band is much broader in the case of the carbonate-containing samples, as hydrogen bonding with interlayer carbonate anions gives rise to the enhanced absorption slightly above 3000 cm⁻¹.^{28,29} The

(22) Gusi, S.; Pizzoli, F.; Triffiró, F.; Vaccari, A.; Del Piero, G.; Delmon, B.; Grange, P. A. In *Preparation of Catalysis IV*; Jacobs, P., Poncelet, G., Eds.; Elsevier: Amsterdam, 1987; p 753.

(23) Del Piero, G.; Di Conca, M.; Triffiró, F.; Vaccari, A. in *Reactivity of Solids*; Barret, P., Dufour, L., Eds.; Elsevier: Amsterdam, 1985; p 1029.

(24) Fuda, K.; Suda, K.; Matsunaga, T. *Chem. Lett.* 1993, 1479.

(25) Martín Labajos, F. M. Ph.D. Thesis. University of Salamanca, 1993.

(26) Clause, O.; Gazzano, M.; Triffiró, F.; Vaccari, A.; Zatorski, L. *Appl. Catal.* 1991, 73, 217.

(27) Cavani, F.; Clause, O.; Triffiró, F.; Vaccari, A. *Adv. Catal. Des.* 1991, 186.

(28) Bish, D. L.; Brindley, G. W. *Amer. Mineral.* 1977, 62, 458.

(29) Kruissink, E. C.; van Reijden, L. L.; Ross, J. R. H. *J. Chem. Soc., Faraday Trans. 1* 1981, 77, 649.

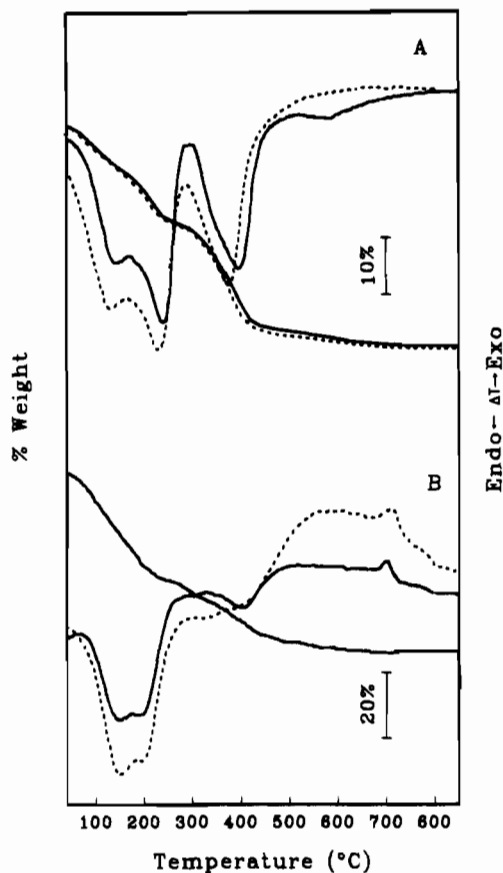


Figure 4. Thermogravimetric and differential thermal analysis curves: (A) sample $\text{MgCrCO}_3\text{-D}$; (B) sample MgCrV . Key: Solid lines, curves recorded in air; dotted lines, curves recorded in nitrogen.

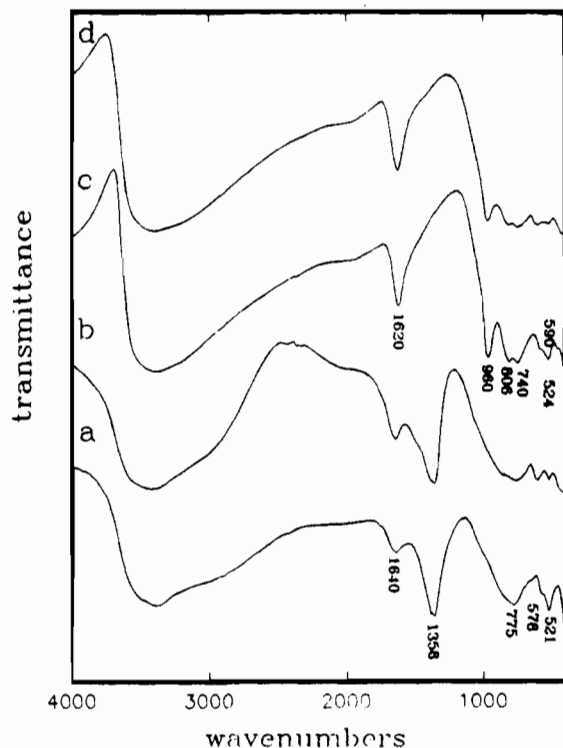


Figure 5. FT-IR spectra of samples (a) $\text{NiCrCO}_3\text{-D}$, (b) $\text{MgCrCO}_3\text{-D}$, (c) NiCrV , and (d) MgCrV .

water deformation band is recorded in all four cases at $1630 \pm 10 \text{ cm}^{-1}$.

The most relevant information provided by these spectra correspond to the presence of the band originated by ν_3 mode

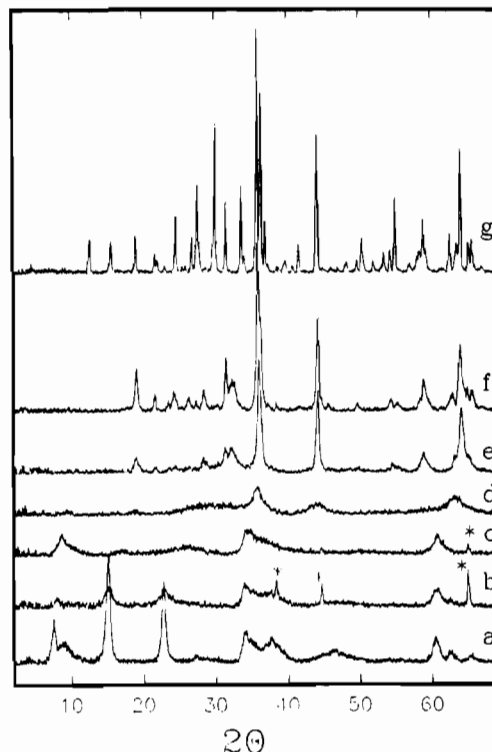


Figure 6. PXRD diagrams for sample NiCrV calcined at (a) 25, (b) 150, (c) 200, (d) 300, (e) 500, (f) 600, and (g) 850 °C. (* = peaks due to the Al sample holder.)

of interlayer carbonate species close to 1360 cm^{-1} .³⁰ Restricted geometry in the interlayer region shifts this band from 1450 cm^{-1} for free carbonate. The band is absolutely absent in the spectra of the decavanadate-containing samples, thus confirming a $\text{CO}_3^{2-}/\text{V}_{10}\text{O}_{28}^{6-}$ exchange under the experimental conditions used. Instead, a series of bands are recorded below 960 cm^{-1} that, according to previous data,^{31,32} are ascribed to decavanadate species. These bands have been also reported by us^{8,12} for decavanadate-exchanged LDHs. Therefore, the band at 960 cm^{-1} can be attributed to the symmetric stretching mode of the terminal $\text{V}=\text{O}$ groups ($\nu_{\text{V}=\text{O}}$),³³ while the bands between 800 and 500 cm^{-1} may be assigned to antisymmetric and symmetric stretching modes of $\text{V}-\text{O}-\text{V}$ chains.³⁴

Thermal Stability. One of the most promising uses of LDHs and POM-intercalated LDHs is as precursors for selective oxidation catalysts. The decomposition patterns of POM-intercalated LDHs to yield mixtures of metallic oxides are therefore important. The solids were calcined at increasing temperatures in air for 3 h, and the PXRD profiles are shown in Figures 6 and 7 for derivatives of samples $\text{Ni}-\text{Cr}-\text{V}$ and $\text{Mg}-\text{Cr}-\text{V}$, respectively.

Calcination of sample $\text{Ni}-\text{Cr}-\text{V}$ at 150 °C leads to a general decrease in the intensities of the diffraction maxima, although their positions remain unaffected; i.e., no important change in the gallery height should occur, and hence the decavanadate moiety should remain unaltered.

Calcination at 200 °C , however, gives rise to changes in the profile. So, the peaks due to decavanadate-intercalated LDH are removed and instead a new, fairly broad, peak develops at 10.12 Å . It should be noted that the (110) peak at 1.53 Å

(30) Hernandez-Moreno, M. J.; Ulibarri, M. A.; Rendon, J. L.; Serna, C. *J. Phys. Chem. Miner.* **1985**, *12*, 34.

(31) Fuchs, J.; Mahjour, S.; Palm, R. *Z. Naturforsch.* **1976**, *B31*, 537.

(32) Salinas, E. L.; Ono, Y. *Bull. Chem. Soc. Jpn.* **1992**, *65*, 2465.

(33) Frederickson Jr, L. D.; Hansen, D. M. *Anal. Chem.* **1978**, *23*, 93.

(34) Griffith, W. P.; Lesniak, J. B. *J. Chem. Soc. A* **1969**, 1066.

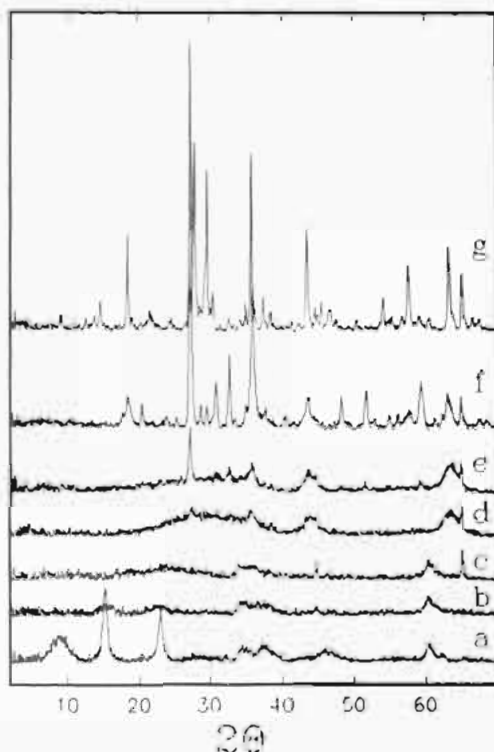


Figure 7. PXRD diagrams for sample MgCrV calcined at (a) 25, (b) 150, (c) 200, (d) 400, (e) 500, (f) 600, and (g) 850 °C. (* = peaks due to the Al sample holder.)

remains, thus suggesting that the material responsible for this pattern is still lamellar and somewhat related to the original material. According to the results reported by Twu and Dutta,³⁵ the peak at 10.12 Å would correspond to diffraction by planes (003) of $V_3O_9^{3-}$ -intercalated LDH.

Calcination at 300 °C destroys completely the layered structure. No indication of any vanadium-related intercalated material exists; weak peaks are recorded at 2.51, 2.05, and 1.47 Å; these should correspond to the oxides of the cations existing in the sample (NiO gives rise to a diffraction peak at 2.05 Å), and the peak at 1.53 Å is no longer seen.

The profile remains unchanged upon calcination at 400 °C (pattern not shown in the figure), but calcination at 500 °C leads to deep changes in the diffraction profile: The peaks that start to develop when the sample had been calcined at 300 °C are now extremely sharp, and when the sample is finally calcined at 850 °C, a general sharpening of all peaks is observed. Interaction between Ni, V, and Cr in the sample leads to formation of $Ni_3V_2O_8$ upon calcination at 300–500 °C, an increase in the calcination temperature leads to development of diffraction peaks originated, in addition, by traces of $Ni_2V_2O_7$, and finally, calcination at 850 °C permits detection of chromia.

The patterns corresponding to calcined products derived from the sample Mg–Cr–V are shown in Figure 7. The behavior is similar to that above shown by the sample Ni–Cr–V: calcination at 150 °C leads to a general decrease of the peak intensities; a general loss of crystallinity is observed upon calcination at 200 °C, no sharp change is observed upon calcination at 300 °C (pattern not shown in the figure), and calcination at 400 °C again gives rise to changes in the diffraction profile.

Calcination at 500 °C gives rise to development of a sharp peak at 3.26 Å that can be ascribed to the presence of $Mg_3V_2O_8$. This is confirmed by the pattern recorded for the sample calcined at 600 °C, which peaks are due to the presence of $Mg_3V_2O_8$

(35) Twu, J.; Dutta, P. K. *J. Catal.* 1990, 124, 503.

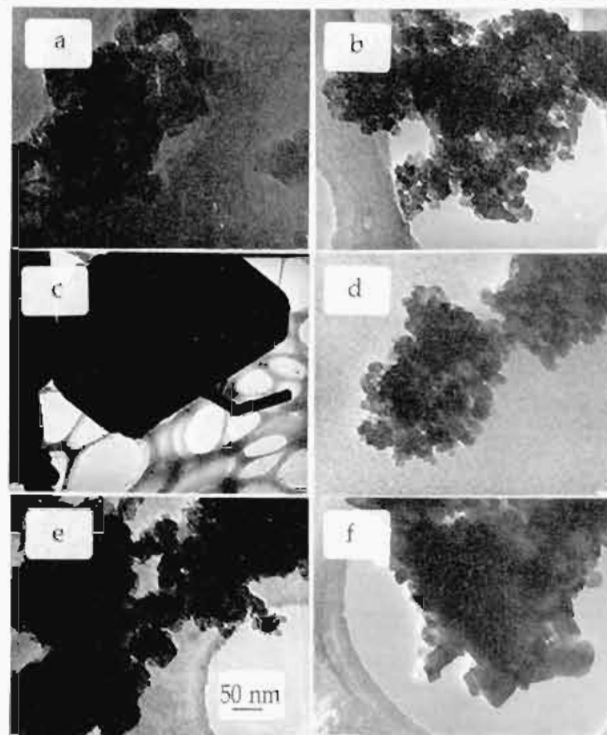


Figure 8. Transmission electron micrographs: (a) NiCrCO₃-D; (b) NiCrV; (c) NiCrV calcined at 700 °C; (d) MgCrCO₃-D; (e) MgCrV; (f) MgCrV calcined at 700 °C.

and also $MgCr_2O_4$. Finally, calcination at 850 °C leads to formation of $Mg_2V_2O_7$ as the major component, together with the $MgCr_2O_4$ spinel phase, $Mg_3V_2O_8$ being now a minor component of the mixture.

As previously reported, stability of supported decavanadate depends on the nature of the support.^{36,37} The structural integrity is maintained up to 450 °C when decavanadate is supported on alumina, but the interlayer space of LDHs seems to provide a more reactive environment and, in the case of Mg,Al-intercalated with decavanadate, even a gentle warming gave rise to decomposition.³⁵ Nevertheless, the nature of the cations present in the host lattice seem also to play a role on the stability of the intercalated decavanadate. As previously reported,¹² in the presence of Ni,Al LDH structural integrity is maintained even up to 300 °C, but as is here shown here, it is destroyed even at 150 °C with hosts containing Ni,Cr or Mg,Cr. According to Twu and Dutta,³⁵ such decavanadate decomposition is related to polarization interactions between water molecules in the interlayer space and the decavanadate moiety, leading to polymers with lower charge density. The presence of cations with different polarizing power in the brucite-like layers would also modify the interaction between the water molecules and the decavanadate anions.

FT-IR monitoring of the thermal decomposition yields conclusions similar to those described above from X-ray diffraction studies.

Transmission Electron Microscopy. Microphotographs for representative samples are included in Figure 8. Sample NiCrCO₃ forms hexagonal platellets, as expected for hydroxalcalite-like particles.^{38,39} However, sample MgCrCO₃ forms aggregates of very small particles.

(36) Roozeboom, F.; Medema, J.; Gellings, P. J. G. *Z. Phys. Chem.* 1978, 111, 215.

(37) Coustumer, L. R.; Taouk, B.; le Meur, M.; Payen, E.; Guelton, M.; Grimblot, J. *J. Phys. Chem.* 1988, 92, 1230.

(38) Uljbarri, M. A.; Fernandez, J. M.; Labajos, F. M.; Rives, V. *Chem. Mater.* 1991, 3, 626.

When decavanadate is incorporated into the interlayer space, both samples Ni–Cr–V and Mg–Cr–V display hexagonal-shaped particles. Calcination at increasing temperatures in air destroys the structure and finally, when calcination is performed at very high temperatures (700 °C or above) a bimodal distribution of particles is observed. The particles are rather large, especially for sample Ni–Cr–V calcined at 700 °C, and the presence of intergrown crystals with different shapes can be tentatively ascribed to the presence of different phases in these samples, as already shown by X-ray diffraction (see above).

Surface Area and Porosity. Nitrogen adsorption isotherms for decavanadate-containing samples correspond to type II in IUPAC's classification, corresponding to unrestricted adsorption on nonporous or macroporous solids,⁴⁰ although a type H2 hysteresis loop is also shown. The specific surface area for sample Ni–Cr–V was 132 m²/g, a value ca. 50% lower than that measured for the carbonate-containing material, NiCrCO₃, 210 m²/g, probably due to the blocking of pores. This result means that porosity does not arise from internal surface, as in such a case it would be expected to yield a larger value for the pillared material than for the carbonate-containing one.²

Changes in specific surface area as the calcination temperature of the decavanadate-containing samples increases are shown in Figure 9. Both series of samples show similar trends, with a decrease in the specific surface area as the calcination temperature increases. In both cases, the average pore diameter increases steadily as the specific surface area decreases.

Conclusion

Exchange of carbonate for decavanadate in Ni,Cr and Mg,Cr anionic clays has been achieved by anionic exchange. A coproduct was always obtained, especially for the Mg-containing sample. The nature of the intercalated polyvanadate was not modified by the pH during anionic exchange. The pH range

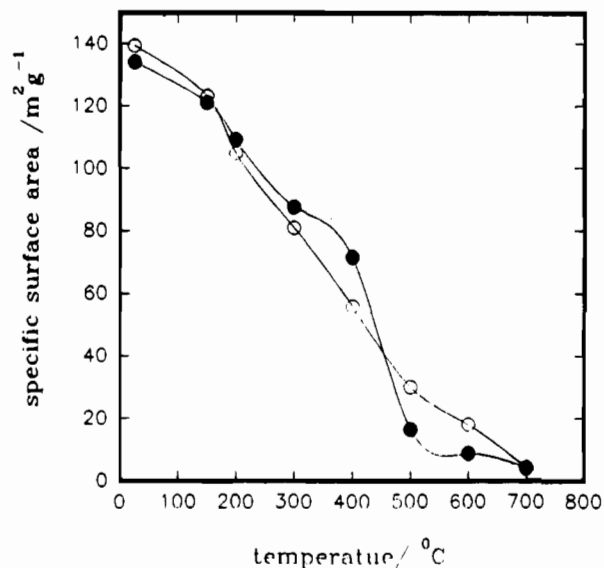


Figure 9. Change in the specific surface area with the calcination temperature for sample NiCrV (solid symbols) and MgCrV (open symbols).

where exchange was successful depends on the divalent cation in the brucite-like layers. No exchange was achieved for sample Mg,Cr at pH > 6.5, but exchange was observed at pH > 5.5 for the sample Ni,Cr. Decavanadate in the interlayer is highly reactive, decomposing to V₃O₉³⁻ upon calcination at 150 °C; further calcination led to a steady decrease in the specific surface area, with formation of highly crystalline Ni (or Mg)–V–O compounds, as characterized by powder X-ray diffraction.

Acknowledgment. F.K. acknowledges a grant from Ministerio de Educación y Ciencia (Madrid, Spain, ref. SB92-AE0474743) and M.A.U. acknowledges a grant from Universidad de Córdoba. Grants from CICYT (MAT91-767 and MAT93-787) and Consejería de Cultura y Turismo (Junta de Castilla y León) are also acknowledged.

IC9500218

(39) Fernandez, J. M.; Barriga, C.; Ulibarri, M. A.; Labajos, F. M.; Rives, V. *J. Mater. Chem.* **1994**, *4*, 1117.

(40) Sing, K. S. W.; Everett, D. H.; Haul, R. A. W.; Moscou, L.; Pierotti, R.; Rouquerol, J.; Siemianowska, T. *Pure Appl. Chem.* **1985**, *57*, 603.